[illegible]

MASTER

ABSTRACT

The topology of all [illegible] center orbits [illegible] displayed in a three-dimensional constants-of-motion space. The treatment is perfectly general and holds for arbitrary axisymmetric MHD equilibria. We show that significant topological changes [illegible] in the [illegible] which are associated with a region of absolute minimum [illegible] in the plasma.

I. Introduction

Detailed knowledge of tokamak particle orbits is essential for understanding neutral beam or α-particle heating, [illegible] electron [illegible], and the basis for all of neoclassical theory. The usual small Banana width treatment of these orbits is inadequate for the description of superthermal particles, and a rigorous, systematic treatment is needed. Furthermore, this treatment should apply to the noncircular, high-β equilibria which are becoming increasingly more studied.

Because each tokamak guiding center orbit can be uniquely specified by three constants of motion (COM), it is logical to represent it as a point in a three-dimensional COM space. This space is divided into regions which denote a particular type of orbit (trapped, circulating, etc.). Thus, given three COM we can distinguish which type of orbit a particle is on and how it can scatter to other regions.

Usually, the three COM's that one associates with an orbit are the energy (ϵ), the magnetic moment (μ), and the toroidal canonical angular momentum (p_ϕ). However, for our purposes, it is preferable to choose the speed (v), the maximum value of the poloidal flux function along the orbit (ψ_m), and the value of $v_\parallel/v$ at this point (ξ), $v_\parallel$ being defined as parallel to $\underline{B}$. Because the orbit is associated with the direction of the plasma current and not the direction of B_ϕ, we give ξ the sign of $\bar{v}\cdot\bar{J}_\phi$. There are many reasons for this selection; the two velocity-like variables, v and ξ, are orthogonal; the space-like variable ψ_m is easily interpreted and has the nice property that if $\psi_m > \psi_{wall}$, the particle is in the loss region; and, most importantly, each orbit maps one-to-one onto the points in this COM space.

In the remainder of this paper, we derive a convenient form of the orbit equation and then describe the various topological features in the new COM space.

II. The Orbit Equation

Because the topological features of the v, ξ, ψ_m space are most easily seen at high energies, we will treat the guiding center orbits relativistically. To be specific, we will treat ion orbits. Although p_ϕ is exactly conserved for the particle orbit it is only conserved through first order for the guiding center [1]:

$$p_\phi = \gamma m R v_\phi - Ze\psi = \text{constant}. \tag{1}$$

Here Z is the charge number of the ion, $\gamma = (1-(v/c)^2)^{-1/2}$, R is the distance to the summetry (Z) axis, and ψ is defined so that it is zero at the magnetic axis and increases nomotonically to a value ψ_w at the wall or limiter.

For ideal MHD equilibria, RB_ϕ is only a function of ψ:

$$RB_\phi \equiv F(\psi). \tag{2}$$

From conservation of μ and ε, we may write $v_\parallel$ at any point along the orbit as

$$v_\parallel = \pm v \sqrt{1-(1-\zeta^2)\frac{B}{B_m}}\ . \tag{3}$$

The subscript m represents values at $\psi = \psi_m$.

Using Eqs. (2) and (3) in Eq. (1) and evaluating Eq. (1) at ψ_m and at a general point along the orbit, we can solve for $B(\psi)$ along the orbit:

$$B = \frac{1}{\frac{1-\zeta^2}{2} + \sqrt{\left(\frac{1+\zeta^2}{2}\right)^2 + \frac{1}{\hat{F}^2}\left[\zeta - G_m(1-\hat{\psi})\sqrt{\frac{c^2}{v^2} - 1}\right]^2}} \tag{4}$$

The dimensionless parameter G_m is given by

$$G_m = \frac{ZeB_m\psi_m}{mcF_m}\ , \tag{5}$$

and all quantities with a circumflex are normalized to their values at $\psi = \psi_m$ along the orbit.

Equation (4) is remarkable in that the right-hand side is only a function of ψ and the COM (v, ζ, and ψ_m). Because the orbit may be regarded as a competition between motion along a field line and the gradient and curvature drifts, ψ will vary monotonically from ψ_m to ψ_n (the minimum value of ψ along the orbit) on both the top half or bottom half of the orbit provided there is up-down symmetry with respect to the (single) magnetic axis. In this paper we only consider the top half of the orbit so that ψ may be used as a running variable along the orbit, and for any such ψ, Eq. (4) will give the value of B. Thus, knowledge of the ψ = constant and B = constant contours is all we need to know to describe an orbit in the poloidal plane. Indeed, the ψ = constant and B = constant surfaces make a very natural coordinate system for orbit considerations, and this explains why they occur in many neoclassical theory formulas.

Furthermore, we note that the only information about the equilibria that is used to describe the orbits is the values of B and F as functions of ψ in the equatorial plane. In this paper, these quantities have been obtained from the Oak Ridge Equilibrium Code [2] for a D-shaped plasma the size of TNS, a prototype ignition device. Figure 1 shows typical α-particle orbits for $\bar{\beta}$ = 1.3% and 7.7% and typical $|B|$ contours. In the high-β case, as will be shown later, an important change in the topology occurs because B has a local maximum on the equatorial plane outside the magnetic axis. This allows the existence of orbits which are different from those of the low-β case.

III. Orbit Topology

Equations for the topological surfaces in the COM space can be derived from Eq. (4) and in most cases can be solved explicitly for v as a function of ζ and ψ. However, due to space considerations, in this paper we only discuss the results and their physics content. The details of this will be presented elsewhere [3].

GUIDING CENTER ORBITS FOR ALPHAS

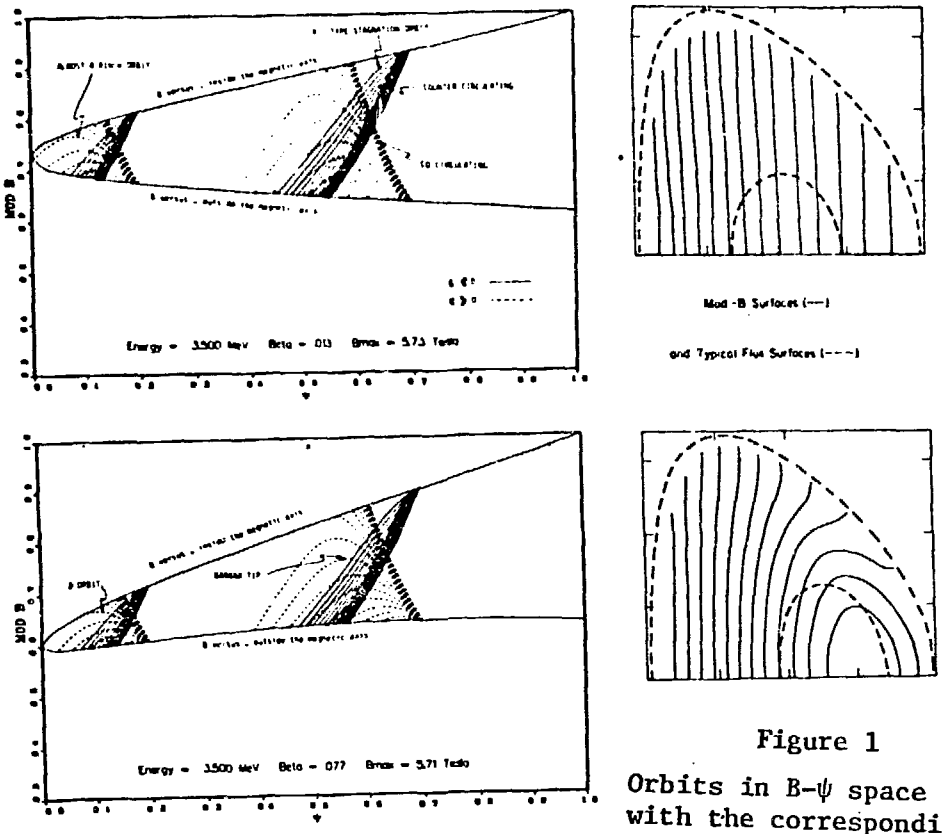

Figure 1

Orbits in B-ψ space along with the corresponding B and ψ contours in real space.

Figure 2 shows all of the relevant topological surfaces for low β and high β. For clarity, we have separated them into their component parts. Figure 2a shows the boundary of the trapped particle region. This is determined by the locus of particles which have $v_{\parallel} = 0$ in the equatorial plane. These orbits are a limit of the usual banana orbits and are D-shaped. Particles lying below this surface are trapped. Because of the uniqueness properties of our space, trapped particles are defined only once for positive values of ζ. Note that in the low-β case, if the particle energy is high enough, there can be no trapped particles because the particle drifts ($\sim v^2$) will always dominate the motion along the field line ($\sim v$). Also, contrary to usual belief, those particles with pitch angles of 90° on the equator are barely trapped, not deeply trapped. In the high-β case, the two disconnected parts of the trapping boundary are due to the local maximum in B. Particles lying between the two regions are still trapped, but the boundary of the region is determined by one of the surfaces to be described later.

The remaining surfaces are all determined by "stagnation point" orbits, which have the property that the particle may remain forever at one location in the poloidal plasma cross section. These "singularities" occur in the equatorial plasma are caused by a cancellation of the $\overline{B} \times \nabla B$ and curvature drifts with the vertical component of $v_{\parallel}$. This is most easily done by setting $dp\phi/dR = 0$ on the equator [1]. The particle can then move only toroidally.

Stagnation points may be either stable (O-type) or unstable (x-type) with respect to small displacements away from the stagnation point. The locus of the stagnation points is important because it determines the maximum velocity boundary of v-ζ-ψ_m space. Since x-type stagnation points have an infinite bounce time, such particles are dominated by collisional effects.

Figure 2b shows the locus of stagnation orbits which have ψ_m on the inside of the magnetic axis. An important feature of this surface is the line which marks the transition from O-type to x-type stagnation orbits. The x-type

Orbit Topology in the Constants-of-Motion Space

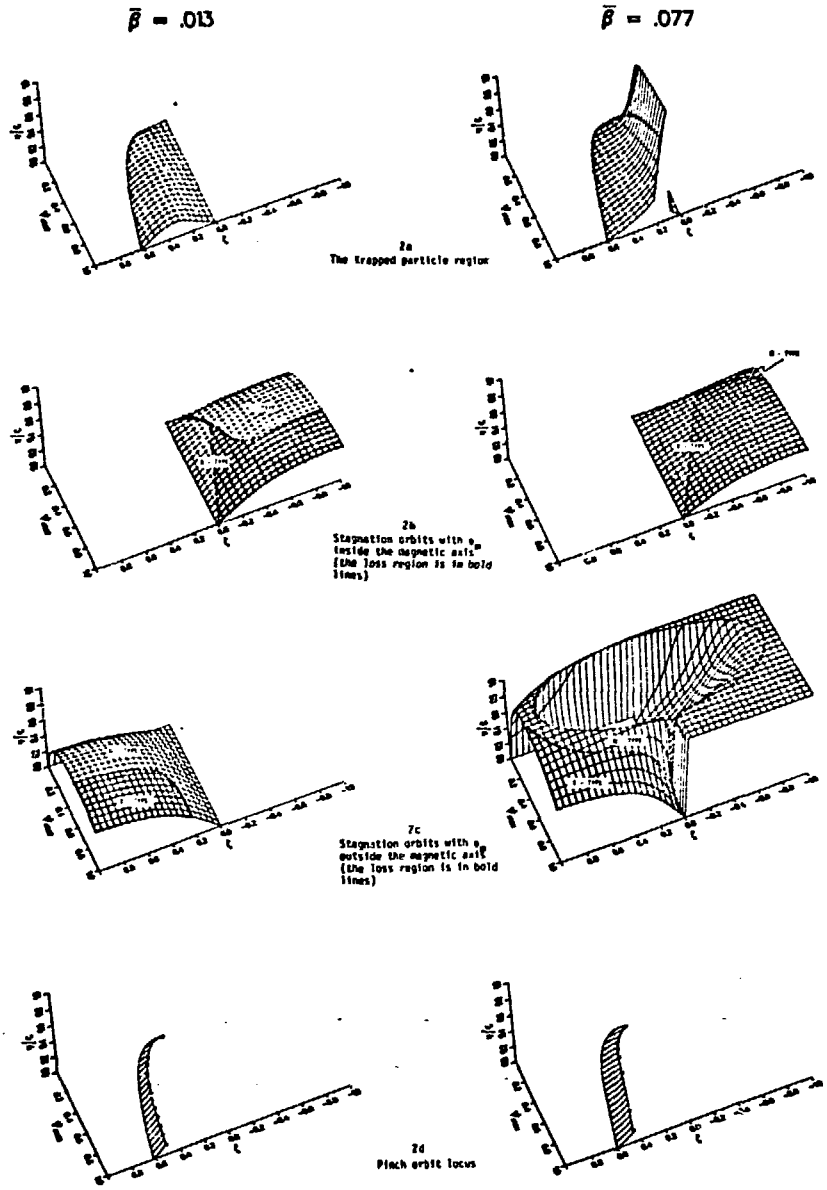

Figure 2

orbits may scatter into fat banana (pinch) orbits (Fig. 3; to be discussed below) which hit the wall, and so part of the x-type locus constitutes a "logs region" (denoted by bold lines). No particles are allowed immediately above this surface because it would correspond to defining ζ at ψ_n instead of ψ_m or to a ψ_m outside of the plasma boundary. Thus, the stagnation orbit locus in the COM space serves to preserve the uniqueness of our orbit representation.

In Fig. 2c we see the locus of stagnation orbits with ψ_m on the outside of the magnetic axis. In this case, all of the X-type orbits may scatter onto orbits which intersect the wall; hence the entire -type orbit region is also the boundary of the loss region. Because this region occurs at high energy, it may be important for runaway electrons which may be accelerated through this boundary.

For the high-β case, the topology is drastically changed in the region where $dB/d\psi > 0$. In this case, the stagnation point surface goes up to $v/c = 1$, and a new class of countergoing untrapped orbits appears above the surface in the $\zeta < 0$ half of space.

We point out the fact that so far, there is no way for a low energy particle to scatter from the $\zeta > 0$ half of space to the $\zeta < 0$ half of space, since there is a forbidden region between them which goes down to $v/c = 0$.

The resolution of this dilemma is provided by a trapped orbit which we call the "pinch orbit" due to the fact that the two banana tips bend down to the equatorial plane and meet in an x-type stagnation point. Once on this orbit, a particle may scatter onto any of three adjacent orbits, as shown in Fig. 3.

Figure 3

ORNL/DWG/FED 78-288

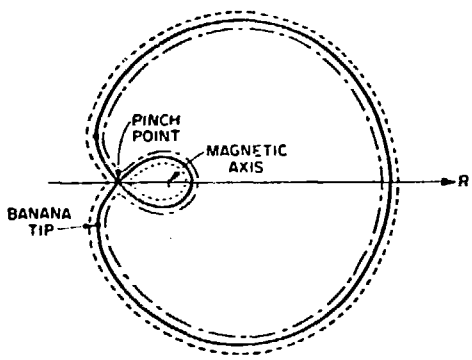

THE PINCH ORBIT AND ITS THREE NEIGHBORING ORBITS.

The innermost of these orbits is an x-type counterstagnation orbit whose locus was shown in Fig. 2b. Thus, by scattering through the pinch orbit, a particle may go from a point with $\zeta > 0$ to a point with $\zeta < 0$ but at a smaller value of ψ_m.

The locus of the pinch orbits is shown in the last part of Fig. 2. This locus lies just inside the trapping region and maps onto the confined orbit part of the x-type stagnation orbit surface of Fig. 2c.

Conclusions

We have developed a systematic picture of the orbit topology based on the COM space to display the loss regions. This is expected to enable us to do beam deposition calculations and to solve the general beam slowing down problem with the Fokker-Planck equation in noncircular two-dimensional MHD equilibria. Since the fast ions are collisionless, the Fokker-Planck equation can be bounce-averaged and still retain the nonlocal, finite banana width, arbitrary β, information that is inherent in the problem. Numerically this is an advantageous procedure since we only need to solve a three-dimensional diffusion problem on a time scale much longer than a bounce time. This is in contrast to solving

a four-dimensional diffusion problem on a time scale much shorter than a bounce time, or to a Monte Carlo treatment.

Acknowledgements

The authors are pleased to acknowledge helpful discussions with Robert Goldston, PPPL, and Lee M. Hively, University of Illinois. Much of the algebraic manipulation required in this paper was performed with the aid of the MACSYMA computer system at M.I.T.

References:

1. T. G. Northrop and J. A. Rome, "Extensions of Guiding Center Motion to Higher Order," Physics of Fluids 21, 384 (1978).
2. R. A. Dory and Y-K. M. Peng, "High Pressure Flux-Conserving Tokamak Equilibria," Nuclear Fusion 17, 21 (1977).
3. J. A. Rome and Y-K. M. Peng, "The Topology of Tokamak Orbits," ORNL/TM-6352 (to be published).